J Ginseng Res 44 (2020) 96–104

Contents lists available at ScienceDirect

Journal of Ginseng Research

journal homepage: http://www.ginsengres.org

Research Article

Oleanolic acid 3-acetate, a minor element of ginsenosides, induces apoptotic cell death in ovarian carcinoma and endometrial carcinoma cells via the involvement of a reactive oxygen species–independent mitochondrial pathway

Hantae Jo [1], Jeong-Hyun Oh [2], Dong-Wook Park [3], Changho Lee [4,**], Churl K. Min [1,*]

[1] Department of Biological Sciences, Ajou University, Suwon, Republic of Korea
[2] Oncology Business Unit, MSD-Korea, Seoul, Republic of Korea
[3] Laboratory of Reproductive Medicine, Cheil General Hospital & Women's Healthcare Center, College of Medicine, Dankook University, Seoul, Republic of Korea
[4] Department of Pharmacology and Biomedical Science, College of Medicine, Hanyang University, Seoul, Republic of Korea

ARTICLE INFO

Article history:
Received 25 May 2018
Received in Revised form
9 September 2018
Accepted 13 September 2018
Available online 19 September 2018

Keywords:
Apoptosis
Endometrial cancer
Oleanolic acids
Ovarian cancer
Reactive oxygen species

ABSTRACT

Objectives: Oleanolic acid, a minor element of ginsenosides, and its derivatives have been shown to have cytotoxicity against some tumor cells. The impact of cytotoxic effect of oleanolic acid 3-acetate on ovarian cancer SKOV3 cells and endometrial cancer HEC-1A cells were examined both *in vivo* and *in vitro* to explore the underlying mechanisms.

Methods: Cytotoxic effects of oleanolic acid 3-acetate were assessed by cell viability, phosphatidylserine exposure on the cell surface, mitochondrial release of cytochrome C, nuclear translocation of apoptosis-inducing factor, depolarization of mitochondrial transmembrane potential ($\Delta\Psi_m$), and generation of reactive oxygen species (ROS). *In vivo* inhibition of tumor growth was also assessed with xenografts in immunocompromised mice.

Results: Oleanolic acid 3-acetate exhibited potent cytotoxicity toward SKOV3 and HEC-1A cells by decreasing cell viability in a concentration-dependent manner. Importantly, oleanolic acid 3-acetate effectively suppressed the growth of SKOV3 cell tumor xenografts in immunocompromised mice. Furthermore, oleanolic acid 3-acetate induced apoptotic cell death as revealed by loss of $\Delta\Psi_m$, release of cytochrome c, and nuclear translocation of apoptosis-inducing factor with a concomitant activation of many proapoptotic cellular components including poly(ADP-ribose) polymerase, *Bcl*-2, and caspases-8, caspase-3, and caspase-7. Oleanolic acid 3-acetate, however, caused a decrease in ROS production, suggesting the involvement of an ROS-independent pathway in oleanolic acid 3-acetate–induced apoptosis in SKOV3 and HEC-1A cells.

Conclusion: These findings support the notion that oleanolic acid 3-acetate could be used as a potent anticancer supplementary agent against ovarian and endometrial cancer. Oleanolic acid 3-acetate exerts its proapoptotic effects through a rather unique molecular mechanism that involves an unconventional ROS-independent but mitochondria-mediated pathway.

1. Introduction

Oleanane triterpenoids, synthesized in many plants including *Panax ginseng* Meyer and widely used in traditional oriental medicine, have been shown to be clinically effective antiinflammatory and antitumorigenic agents [1]. To improve their anticancer potency, some chemical modifications have been introduced, and some are met with positive outcomes [2]. These synthetic oleanane triterpenoids (SOTs) primarily come into play in relation to inflammation, oxidation, proliferation, and apoptosis. Despite

* Corresponding author. Department of Biological Sciences, Ajou University, Suwon 16499, Republic of Korea.
** Corresponding author. Department of Pharmacology and Biomedical Sciences, College of Medicine, Hanyang University, Seoul 04763, Republic of Korea.
E-mail addresses: jennysue@hanyang.ac.kr (C. Lee), minc@ajou.ac.kr (C.K. Min).

https://doi.org/10.1016/j.jgr.2018.09.003
p1226-8453 e2093-4947/$ – see front matter

much effort to elucidate the structure–function relationship of SOTs for the chemoprevention and chemotherapy of cancers, the active moieties that could confer anticancer therapeutics to SOT are currently not known, nor is the molecular target(s) of SOT in cancer prevention. However, SOT and its derivatives offer a very promising anticancer intervention because of their potential to regulate a rather broad range of dysfunctional pathways that are frequently encountered in many types of cancer, highlighting a broad relevance for the cancer control.

Ovarian cancer is one of the high mortality-inflicted gynecological malignancies worldwide [3]. The high mortality associated with ovarian cancer is largely attributable to the sporadic emergence of symptoms in an early stage of disease progression and a paucity of effective screening methods. Not surprisingly, most women are diagnosed in such an advanced stage that the 5-year survival rates are nowhere near as high as 50% while diagnosis made in the early stage being confined to the ovaries leads to significantly increased 5-year survival rate of about 90%. This assessment necessitates an effective early screening/detection method to lower the disease-associated mortality [4]. On the other hand, the nature of cancer genome, e.g., progressive accumulation of multiple mutations in tumor as it progresses, might confer upon ovarian cancer the lack of specific early symptoms and some difficulties met in early diagnosis. Indeed, mutations of more than 100 genes were described in human breast and colorectal cancers [5], and the same might be true in other types of cancer. The present notion is that tumor cells might contain thousands of mutations resulting from stochastic and environmental processes. Consequently, no rate-limiting steps or pathways could be uniquely targeted to deter the progression of tumor [6]. By extrapolation, these findings suggest that the combination chemotherapy is of better use than any single drug-based dosing. Albeit different extents, binding to many individual signaling molecules renders SOT a better chemotherapeutic agent providing higher potential to regulate a variety of defective pathways in premalignant or malignant cells than an agent that may target a specific step in a signaling pathway [7].

Apoptosis is considered a precise self-regulating death-leading process, which plays a central role in controlling development and homeostasis of multicellular organisms. Therefore, its malfunction has been closely associated with various diseases, including cancers and cell-degenerative disorders [8]. The two major apoptotic routes have been recognized: the mitochondria-mediated pathway and the cell surface death receptor–mediated pathway. Of the two, binding of a death receptor ligand to the cell surface death receptor leads to activation of caspase-8 and downstream caspases [9]. In the mitochondrial pathways, internal death cues are finally converted to triggering the depolarization of mitochondrial membrane potential ($\Delta\Psi_m$), which is a prerequisite to the mitochondrial cytochrome c release into the cytosol. Released cytochrome c binds to the apoptotic protease activation factor Apaf-1, subsequently leading to caspase-9 activation. Activated caspase-9 further activates many downstream caspases, which collectively leads to apoptosis [10]. In addition, many studies have reported that some anticancer drugs could trigger cells to produce reactive oxygen species (ROS), which in turn takes part in the mitochondrion-mediated apoptosis by dissipating $\Delta\Psi_m$ [11] while others induce apoptosis through the mitochondrial pathway characterized by ROS independence [12–14].

In the present study, we sought to investigate effects of oleanolic acid 3-acetate, a newly synthesized oleanane-based derivative, on the cytotoxicity against human ovarian cancer SKOV3 cells and endometrial cancer HEC-1A cells, and explore its underlying molecular mechanism whereby cancer cells are apoptotically controlled.

2. Materials and methods

2.1. Chemicals

Followings are the lists of materials used and their manufacturers: (a) 3-(4,5-dimethylthiazol-2-yl)-2,5-diphenyltetrazolium bromide) (MTT), dichloro-dihydro-fluorescein diacetate (DCFH-DA), and $DiOC_6$ were purchased from Sigma-Aldrich (St. Louis, MO); (b) Annexin V fluorecein isothiocyanate (FITC) Apoptosis Detection Kit I was from BD Pharmingen (San Diego, CA); (c) Rabbit polyclonal anti-human antibodies against cleaved caspase-3, caspase-7, caspase-8, poly(ADP-ribose) polymerase (PARP), cleaved PARP, and *Bcl*-2 were from Cell Signaling Technology (Danvers, MA); (d) Rabbit polyclonal anti-human antibodies against cytochrome c, apoptosis-inducing factor (AIF), HSP60, and mouse monoclonal anti-human β-actin were from Santa Cruz Biotech (Santa Cruz, CA); (e) horse radish peroxidase–conjugated anti-rabbit IgG and FITC-conjugated anti-rabbit IgG were obtained from Invitrogen (Grand Island, NY); (f) Roswell Park Memorial Institute (RPMI) 1640 medium, fetal bovine serum (FBS), and other tissue culture supplies were from Gibco-BRL (Grand Island, NY); (g) Mitochondria Isolation Kit for Cultured Cells was from Thermo Scientific (Rockport, IL); (h) Oleanolic acid, oleanolic acid acetate, and oleanolic acid methyl ester were purchased from Sigma-Aldrich, BOC Sciences (Shirley, NY), Extrasynthese (Genay, France), respectively. Oleanolic acetate methyl ester was derived from oleanolic acid methyl ester in the presence of pyridine by reacting with acetic anhydride overnight at room temperature. The chemical identity of oleanolic acetate methyl ester was confirmed by mass spectroscopy (HP 5989B; Agilent Technologies, Santa Clara, CA), IR spectroscopy (FT/IR-4200; JASCO, Oklahoma City, OK), and NMR spectroscopy (GEMINI 2000; Varian Technologies, Palo Alto, CA) spectral analysis. MS:535.56 $(M+Na)^+$, $C_{33}H_{52}O_4$; IR(KBr): 2938,1727,1467, 1322,1238,1202,1029,827,755; NMR($CDCl_3$)^{1}H:2.01(s,CH_3CO),2.83 (dd,J = 11.0,3.0,H-18β), 3.59(s,OCH_3), 4.46 (dd,J = 6.6,6.1,H-3α), 5.22 (t,J = 3.5,H-12) (i) all other chemicals, unless specified otherwise, were from Sigma-Aldrich.

2.2. Cell culture

SKOV3 cell, a human ovarian cancer cell line, and HEC-1A cell, a human endometrial carcinoma cell line, were obtained from the American Type Culture Collection (Manassas, VA) and maintained according to the manufacturer's instruction at 37°C in RPMI 1640 medium supplemented with 100 U/mL of penicillin, 100 μg/mL of streptomycin, and 10% FBS in a humidified incubator in the presence of 5% CO_2. Human endometrial tissues at the proliferative phase were isolated by surgical curettages of the hysterectomized uteri of patients at the Ajou University Hospital (Suwon, South Korea) with no apparent diagnosis of endometrial diseases. Informed consent was obtained from a patient before the surgery following the Ajou University Institutional Review Board preapproval (Suwon, South Korea). From the pooled endometrial tissues, the stromal cell–enriched fractions were isolated and maintained as described previously [15].

2.3. Oleanolic acid 3-acetate treatment and determination of cytotoxicity

Cells in a logarithmic growth phase were harvested and seeded in a 96-well plate at a density of 5×10^3 cells/mL (SKOV3 cells) and 2×10^4 cells/mL (HEC-1A cells) in the final volume of 190 μL/well. After 24-h incubation, 10 μL of oleanolic acid 3-acetate was added to the 96-well plate at the final concentration of 0–40 μM for 24 h.

The viability of each cell was examined by MTT assay as described previously [16]. All the experiments were repeated three to five times, and the average is presented. Cell survival was calculated according to the following formula: survival (%) = experimental absorbance/control absorbance × 100.

2.4. Flow cytometric assessment of phosphatidylserine exposure on the cell surface

The extent of phosphatidylserine exposure on the cell surface membrane was one of the hallmarks to quantify early apoptosis by flow cytometry with FITC–Annexin V binding as described previously [17]. In short, about 6×10^5 cells were seeded in a 25-cm^2 flask dish and allowed to attach to the surface of the dish for 24 h. After treatment with oleanolic acid 3-acetate for 24 h, both floating and nonfloating cells were harvested, washed with ice-cold phosphate-buffered saline (PBS) twice, resuspended in 200 μL of 1 × binding buffer containing FITC Annexin V at 1:50 dilution and 40 ng/sample of propidium iodide (PI), and incubated for 15 min at 37°C in the dark. The number of apoptotic cells were quantified by a flow cytometer (model FACSCaliber, BD Bioscience, Franklin Lakes, NJ) with excitation at 488 nm and emission at 525 nm for FITC and 610 nm for PI, respectively, and analyzed by CellQuest software (BD Bioscience).

2.5. Assessment of mitochondrial release of AIF

About 5×10^4 cells were seeded on a coverslip in a 24-well plate in RPMI 1640 medium. Twenty four hrs after seeding, oleanolic acid 3-acetate was added at the final concentrations of 0–40 μM for 24 h. The cells on the coverslip were washed once with ice-cold PBS, fixed in 1 mL of 4% paraformaldehyde for 20 min, washed once with ice-cold PBS containing 5% bovine serum albumin to prevent nonspecific bindings, and incubated for 1 h with anti-AIF antibody at a 1:100 dilution. After washing with ice-cold PBS, FITC-conjugated secondary antibody at 1:100 dilution was added and incubated for 1 h followed by replacing the antibody solution with a staining solution containing PI at 100 nM and further incubated for 5 min. After three washes with ice-cold PBS, the coverslip was mounted onto a glass slide using the antifade mounting reagent. The slides were viewed under a confocal laser-scanning microscope (TCS STED; Leica Microsystems, Bannockburn, IL).

2.6. Measurement of mitochondrial transmembrane potential

$\Delta\Psi_m$ was measured by flow cytometry (FACSCaliber) after staining with fluorescent mitochondrial tracking dye $DiOC_6$. After being exposed to oleanolic acid 3-acetate for 24 h, 1×10^6 cells were harvested, centrifuged at 1,000 rpm in a table-top centrifuge for 5 min, washed with ice-cold PBS once, incubated with 40 nM $DiOC_6$ at 37°C for 15 min in the dark, and analyzed by a flow cytometer (FACSCaliber) with excitation at 488 nm and emission at 510 nm after washing with PBS. The data obtained from the flow cytometry were further analyzed by using the CellQuest software and expressed as mean fluorescence intensity.

2.7. Measurement of ROS production

DCFH-DA is a membrane-permeable dye that specifically detects ROS. About 1×10^6 cells were exposed to either 1–40 μM oleanolic acid 3-acetate or 1 mM H_2O_2 for 24 h. Cells were harvested, washed once with ice-cold PBS, and incubated with DCFH-DA at a final concentration of 100 μM at 37°C for 15 min in the dark. After a wash and resuspending in 1 mL of PBS, ROS generation was assessed by a flow cytometer (FACSCaliber) with excitation and emission at 488 nm and 530 nm, respectively. The DCF fluorescence data were further customized by using the CellQuest software and expressed as mean fluorescence intensity.

2.8. Immunoblotting

After being exposed to oleanolic acid 3-acetate for 24 h, cells were harvested by centrifugation, solubilized in the lysis buffer that constitutes 2% Triton X-100 and 0.1% sodium dodecyl sulfate (SDS) dissolved in 150 NaCl, 25 Tris-HCl, pH 7.4 in mM, supplemented with a protease/phosphatase inhibitor cocktail. The total cell lysates were recovered by centrifugation at 15,000×*g* for 30 min. About 30–50 μg of protein lysates was loaded into a well of the SDS–polyacrylamide gel, subjected to separation by electrophoresis, and transferred onto nitrocellulose membranes. The membranes were first incubated in the blocking solution containing 5% skim milk and 0.1% Tween-20 in PBS at room temperature for 1 h and then were further incubated with appropriate primary antibodies diluted in the blocking solution overnight at 4°C. Finally, the membrane blots were incubated with appropriate horse radish peroxidase–conjugated secondary antibodies at 1:3,000 dilution at room temperature for 1 h. Visualization was made by enhanced chemiluminescence using the Western blotting luminol reagent and a luminescent image analyzer (Las-1000; Fuji Film, Tokyo, Japan). All primary antibodies were diluted at 1:1,000 except the mouse monoclonal anti β-actin antibody (1:4,000). For a quantitative comparison, the intensity of immunoblots was quantified using Multigauge V3.0 software (Fuji Film).

2.9. Mitochondrial fractionation

Mitochondria-enriched fractions were isolated from cells using the Mitochondria Isolation Kit for Cultured Cells following the manufacturer's protocol. Briefly, 2×10^7 exponentially growing cells were cultured, treated with oleanolic acid 3-acetate for 24 h, and then harvested by centrifugation. The mitochondrial and cytosolic fractions were prepared from the cells using the reagent-based and Dounce homogenization methods of the kit.

2.10. Ovarian cancer xenografts

Female athymic mice, BALB/c nu/nu, 6- to 8-weeks old, were obtained from Orient Bio (Sungnam, South Korea) and housed in sterile cages at controlled temperature (23 ± 2°C), lighting (12 h), and humidity (60 ± 5%). Food and water were available *ad libitum*. All animal experimental procedures were prereviewed and approved by the Institutional Animal Research Ethics Committee at Ajou University, Suwon, South Korea. Transplantable SKOV3 cells were cultured, harvested, and suspended at a concentration of 5×10^7 cells/mL in PBS. The athymic mice were inoculated subcutaneously (*s.c.*) into the left flank with 5×10^6 SKOV3 cells in 100 μL of PBS as described elsewhere [18]. When the external diameter of tumors reached approximately 0.5 cm, the mice were randomly divided into following five groups: Group 1, treated with 0.1% dimethylsulfoxide (DMSO) in saline; Group 2, treated with cisplatin; and Groups 3, 4 and 5, treated with oleanolic acid 3-acetate at different doses. Administration of a dose comprises: Groups 1 and 2 mice were randomly treated intraperitoneally (*i.p.*) with 50 μL of 0.1% DMSO and cisplatin at 5 mg/kg dosage once a week for 3 weeks, respectively. Groups 3, 4, and 5 mice were treated *i.p.* with 50 μL of oleanolic acid 3-acetate at 10, 20, and 40 mg/kg, respectively, every day for 3 weeks according to the previous study [19]. The weights of animals were measured every 3 days. When receiving the desired drug dosage, each animal was tagged in the ear and monitored individually throughout the

experiment. Starting on the first day of the drug treatment, the volume of the tumor xenografts was assessed every 3 days according to the following formula: with two perpendicular diameters A and B, the tumor volume (V) was estimated as $V = \frac{\pi}{6}\left(\frac{A+B}{2}\right)^3$. The mice were killed by cervical dislocation when the mean tumor weight was more than 1 g compared to controls. Tumors were excised from the mice, and their weight was measured. The ratio of inhibition (IR) was calculated according to the following formula:

$$IR = 1 - \frac{tumor\ weight\ of\ experimental\ animal}{tumor\ weight\ of\ control\ animal} \times 100(\%)$$

2.11. Statistical analysis

The statistical analysis was performed by Student *t* test or one-way analysis of variance with IBM SPSS Statistics 20 (IBM-Korea, Seoul, South Korea). A p value < 0.05 was set to be indicative of significant difference.

3. Results

3.1. Oleanolic acid 3-acetate inhibits proliferation of SKOV3 and HEC-1A cells

We evaluated the cytotoxic effects of oleanolic acid 3-acetate on two tumor cell lines SKOV3 cells and HEC-1A cells. The cells were treated with oleanolic acid 3-acetate at the final concentrations ranging from 0 to 40 μM for 24 h and subjected to MTT assay to evaluate cell viability. Oleanolic acid 3-acetate exhibited anti-cellular proliferation of SKOV3 and HEC-1A cells in a concentration-dependent manner (Fig. 1B), suggesting that oleanolic acid 3-acetate has a cytotoxicity toward SKOV3 and HEC-1A cells with the half maximal inhibitory concentrations estimated to be 8.3 and 0.8 μM, respectively. In contrast, human endometrial stromal cells, which were assumed to a normal counterpart of HEC-1A cells, showed little, if any, cytotoxicity caused by oleanolic acid 3-acetate (~95% cell survival at 10 μM).

3.2. Oleanolic acid 3-acetate induces apoptotic cell death

An assessment of apoptosis was made by measuring the exposure of phosphatidylserine on the cell surface. SKOV3 and HEC-1A cells were exposed to varying concentrations (0–20 μM) of oleanolic acid 3-acetate for 24 h and then subjected to flow cytometric analysis after annexin V and PI double staining. The early apoptotic cell population (annexin V^+/PI^-) in SKOV3 and HEC-1A cells was 3.9 ± 0.5% and 4.9 ± 0.5% in the control (0 μM), 11.5 ± 2.7% and 11.6 ± 2.6% at 5 μM, 22.4 ± 2.4% and 13.8 ± 2.8% at 10 μM, and 26.1 ± 3.8% and 35.9 ± 3.9% at 20 μM oleanolic acid 3-acetate (Fig. 2A and B), indicating that the percentage of apoptotic cell population increases with oleanolic acid 3-acetate concentration.

3.3. Oleanolic acid 3-acetate induces AIF translocation from the mitochondria to the nucleus

AIF is a mitochondrial flavoprotein that is released from the mitochondria in response to intrinsic death stimuli, subsequently

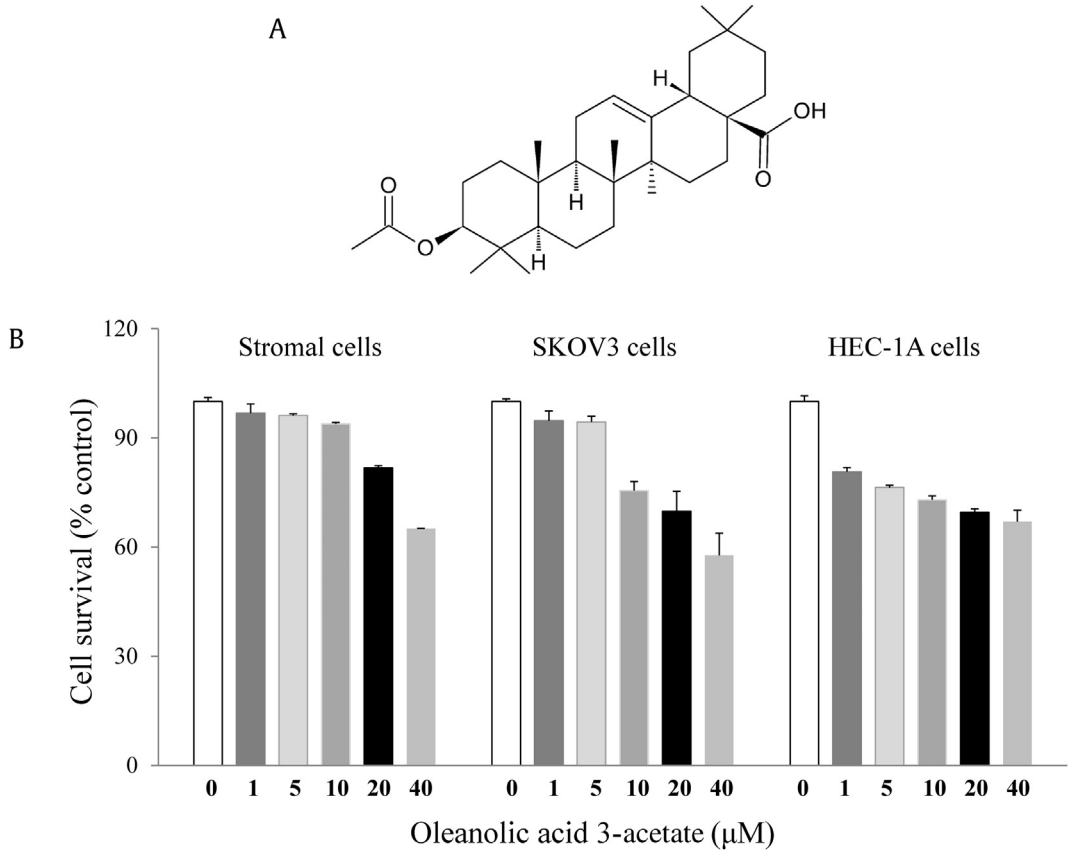

Fig. 1. Oleanolic acid 3-acetate displays cytotoxicity toward SKOV3 and HEC-1A cells. (A) The chemical structure of oleanolic acid 3-acetate. (B) Human endometrial stromal cells, SKOV3, and HEC-1A cells were treated with 0–40 μM oleanolic acid 3-acetate for 24 h, and its cytotoxicity was measured using the MTT assay. Data represent means ± SD of at least triplicate determinations. SD, standard deviation.

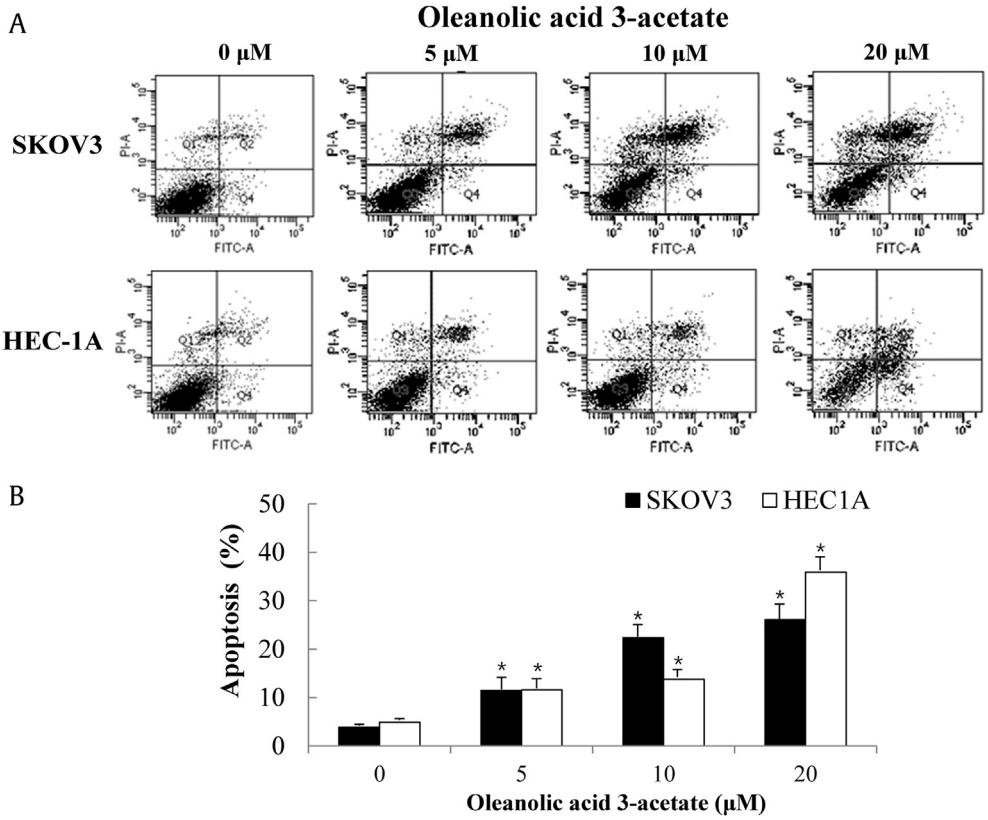

Fig. 2. Oleanolic acid 3-acetate induces apoptotic cell death in SKOV3 and HEC-1A cells. (A) After treatment with oleanolic acid 3-acetate (0–20 μM) for 24 h, both SKOV4 and HEC-1A cells were stained with FITC-conjugated annexin V and propidium iodide (PI) and subjected to flow cytometry. The x-axis represents the fluorescence intensity from FITC, whereas the y-axis represents the fluorescence intensity from PI. Apoptotic cell populations (annexin V^+/PI^-) can be differentiated from normal cells (annexin V^-/PI^-) or necrotic cells (annexin V^-/PI^+) on the basis of their fluorescence intensities. (B) The percentages of apoptotic cell populations in each treatment were plotted. More than 10,000 cells were analyzed in each treatment. The results represented the data of three assays (means ± SD). $^*p < 0.05$ versus control (without oleanolic acid 3-acetate treatment). SD, standard deviation.

translocated into the nucleus before the nuclear DNA condensation ensues [20]. We then tested whether oleanolic acid 3-acetate induced apoptotic cell death through the AIF-mediated pathway. Translocation of AIF into the nucleus was visualized by immunostaining for AIF and PI staining for the nucleus. Our results clearly showed that AIF was released into the cytosol and then translocated into the nucleus after oleanolic acid 3-acetate treatment in a concentration-dependent manner (Fig. 3A), suggesting that AIF release and translocation are involved in the oleanolic acid 3-acetate–induced apoptotic cell death of SKOV3 cells.

3.4. Oleanolic acid 3-acetate induces the loss of mitochondrial transmembrane potential

The loss of $\Delta\Psi_m$ is regarded as one of the hallmarks in apoptotic cell death, and as such, $DiOC_6$ is frequently used as a mitochondrion-specific and voltage-dependent dye for $\Delta\Psi_m$ in living cells. To test for the oleanolic acid 3-acetate–mediated apoptotic pathway, we measured the effect of oleanolic acid 3-acetate on $\Delta\Psi_m$ by flow cytometry. Treating cells with oleanolic acid 3-acetate caused a concentration-dependent decrease in $\Delta\Psi_m$ in both SKOV3 and HEC-1A cells. The portions of $\Delta\Psi_m$ loss due to mitochondrial depolarization were 25.4, 32.6, 36.7, and 47.2% in SKOV3 cells when exposed to 0, 5, 10, and 20 μM of oleanolic acid 3-acetate, respectively, and the corresponding values were 20.1, 22.8, 26.9, and 45.7% in HEC-1A cells (Fig. 3B), suggesting that oleanolic acid 3-acetate induces apoptotic cell death involving, at least, mitochondrial dysfunction.

3.5. Oleanolic acid 3-acetate reduces intracellular ROS production

We then revisited the question of whether ROS production was increased upon oleanolic acid 3-acetate treatment because ROS is regarded as a potential factor related to the mitochondrion-dependent cell injury. Cellular ROS level was determined by flow cytometry using the ROS-sensitive fluorescent probe DCFH-DA. After being exposed to 0–40 μM of oleanolic acid 3-acetate for 24 h, the cellular levels of ROS were 84.3 ± 8.0%, 72.1 ± 11.0%, 65.4 ± 8.1%, 57.9 ± 10.6%, and 54.6 ± 13.3% as relative to control (0 μM) in SKOV3 cells and 80.9 ± 2.9%, 65.8 ± 3.7%, 57.4 ± 4.9%, 53.6 ± 6.9%, and 51.1 ± 2.0% in HEC-1A cells, respectively (Fig. 3C). Note that the ROS level was increased when cells were exposed to 1 mM H_2O_2 with 199.8 ± 30.0% and 217.9 ± 19.4% relative to control in SKOV3 and HEC-1A cells, respectively (data not shown). These findings strongly suggest that oleanolic acid 3-acetate induces apoptotic cell death in SKOV3 and HEC-1A cells but in an ROS-independent manner.

3.6. Oleanolic acid 3-acetate activates a mitochondrial apoptotic pathway and its downstream signaling components

To explore the underlying apoptotic pathway associated with the response of cells to oleanolic acid 3-acetate, we examined the activation states of signaling components downstream of the mitochondrial apoptotic pathway. Oleanolic acid 3-acetate treatment led to the activation of several apoptotic signaling molecules including caspase-3, caspase-7, caspase-8 and their substrate

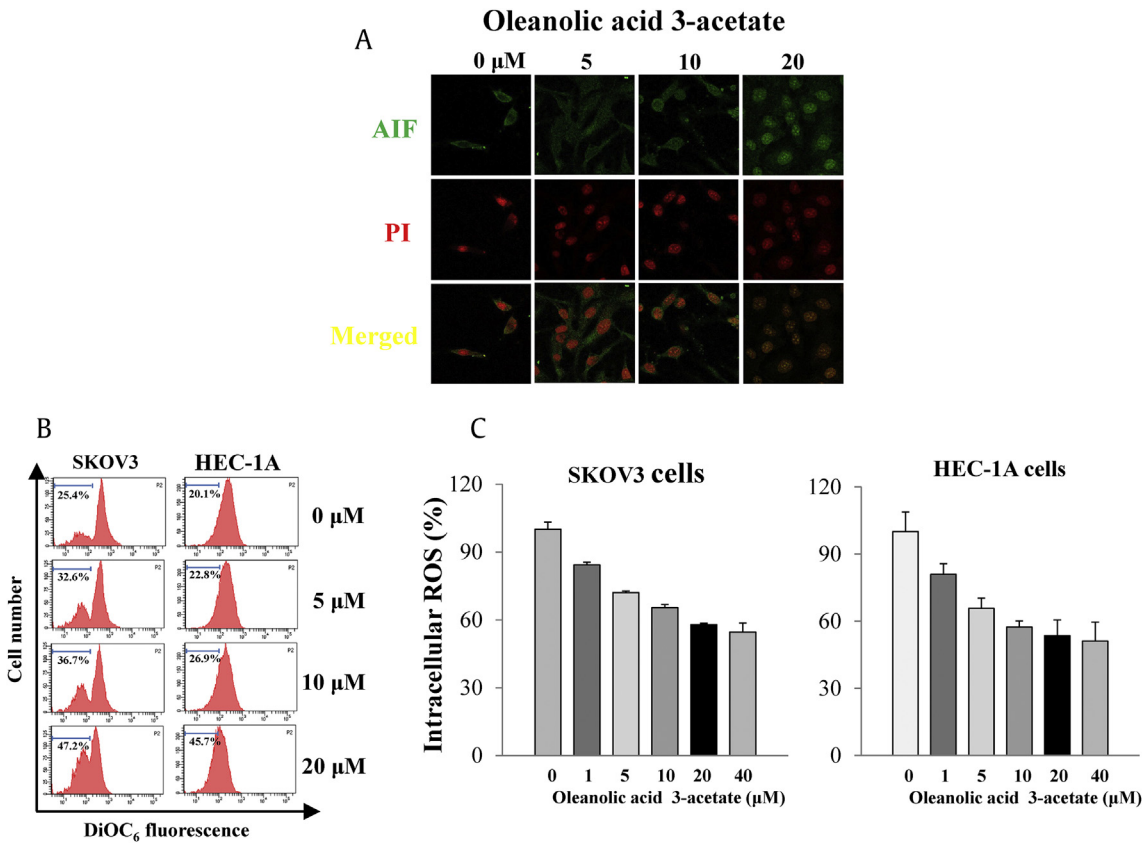

Fig. 3. Oleanolic acid 3-acetate induces apoptotic cell death via mitochondria-mediated signaling. (A) SKOV3 cells were treated with oleanolic acid 3-acetate (0–20 μM) for 24 h. AIF and the nucleus were fluorescently labeled with anti-AIF antibodies (green) and propidium iodide (red), respectively. Shown were representative confocal images. (B) SKOV3 cells and HEC-1A cells were exposed to 0–20 μM oleanolic acid 3-acetate for 24 h. $\Delta\psi_m$ was analyzed by flow cytometry after staining with mitochondrial transmembrane potential–sensitive fluorescent dye $DiOC_6$. The x-axis represents the fluorescent intensity from $DiOC_6$, in a logarithmic scale, and the y-axis represents the cell number. The percentage of mitochondrial membrane potential loss due to depolarization is calculated as percentage loss in fluorescence intensity. Data were representatives of at least triplicate determinations. (C) SKOV3 cells and HEC-1A cells were preloaded with DCFH-DA and further stimulated with oleanolic acid 3-acetate (0–40 μM) for 24 h. The ROS production was analyzed by flow cytometry owing to the fluorescence from DCFH-DA. The ROS level was calculated as percentage of the control (without oleanolic acid 3-acetate treatment). Data were represented as means ± SD of at least triplicate determinations. AIF, apoptosis-inducing factor; PI, propidium iodide; SD, standard deviation.

PARP in a concentration-dependent manner while a dramatic reduction in *Bcl*-2 level, a major antiapoptotic regulator, was manifested (Fig. 4A). The mitochondrial apoptotic pathway is characterized by cytochrome c release from the mitochondria into the cytoplasm concomitant with the loss of $\Delta\Psi_m$ [21]. To differentiate mitochondrial cytochrome c from cytoplasmic cytochrome c, immunoblotting was performed with cytoplasmic and mitochondrial soluble fraction obtained from HEC-1A cells after oleanolic acid 3-acetate treatment. The concentration-dependent accumulation of cytochrome c in the cytosol and corresponding disappearance from the mitochondria were observed along with AIF, implying cytochrome c and AIF release from the mitochondria to the cytoplasm is accelerated upon oleanolic acid 3-acetate treatment (Fig. 4B–D). Taken together, the data clearly demonstrate that oleanolic acid 3-acetate induces apoptotic cell death in an ROS-independent but mitochondria-mediated pathway.

3.7. Oleanolic acid 3-acetate inhibits growth of SKOV3 cell xenografts in nude mice

To further validate oleanolic acid 3-acetate antitumor activity in a cell culture model, we then sought to investigate its antitumor effects in a xenograft mouse model of ovarian cancer. First, we established SKOV3 cell xenografts in nude mice by injecting SKOV3 cells into the frank. After 3 weeks of growth, the external tumor size became visible with an average diameter of 0.5 cm. Then, the mice were randomly divided and subjected to a daily *i.p.* injection of oleanolic acid 3-acetate for the next 19 days. The first group of mice received a vehicle solution (0.1% DMSO diluted in saline), and the second group of mice received cisplatin at a dose of 5 mg/kg body weight. The last 3 groups of mice received oleanolic acid 3-acetate at a dose of 10, 20, and 40 mg/kg body weight, respectively. The tumor volume was measured every 3 days, and the mice were sacrificed at the end of the experiment to excise tumors, and their weights were measured. The tumor volume was steadily increased by 3.5 folds from approximately 1.0 cm^3 at day 1 to 3.5 cm^3 at day 19 without any oleanolic acid 3-acetate treatment. The daily treatment of oleanolic acid 3-acetate suppressed the tumor growth in a dosage-dependent manner, and at the highest dosage used (40 mg/kg), the tumor growth was suppressed by as much as 23% (Fig. 5A and B). The tumor weight also revealed the antitumoral effect of oleanolic acid 3-acetate such that the tumor weight was 2.19 ± 0.88 g in the vehicle control, whereas those were 1.48 ± 0.46, 1.35 ± 0.39, and 1.18 ± 0.38 g at a dose of 10, 20, and 40 mg/kg, respectively ($p < 0.05$) (Table 1). Accordingly, the corresponding tumor growth inhibition ratios were 32.50, 38.47, and 46.02%, respectively. Importantly, oleanolic acid 3-acetate did not cause any death and weight loss in the concentration range used (Table 1),

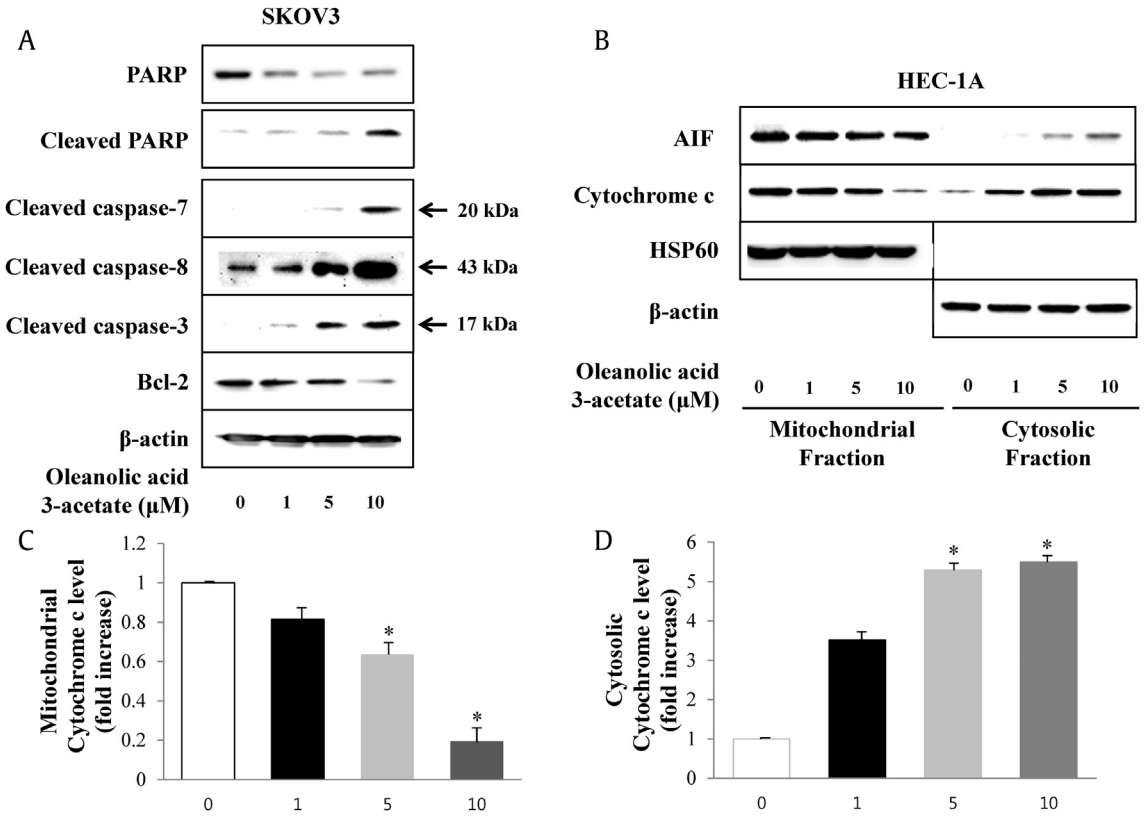

Fig. 4. Oleanolic acid 3-acetate induces the release of cytochrome c and AIF from the mitochondria with a concomitant activation of caspase-3, caspase-7, caspase-8, and PARP in SKOV3 and HEC-1A cells. SKOV3 and HEC-1A cells were exposed to the indicated concentration of oleanolic acid 3-acetate for 24 h. (A) Total cell lysates were subjected to Western blot analysis with the specific antibody against PARP, cleaved PARP, cleaved capase-7, cleaved caspase-8, cleaved caspase-3, *Bcl*-2, and β-actin. β-Actin was used as a loading control. (B) The (C) cytosolic fractions and (D) mitochondrial fractions were separated and subjected to Western blot analysis for AIF, cytochrome c, HSP60, and β-actin. The bars represent the results of densitometric analysis of band intensities in (B) corresponding to mitochondrial and cytosolic cytochrome c by using MultiGuage software. Data were normalized to control and presented as means ± SD of at least triplicate determinations. $^{*}p < 0.05$ versus control (without oleanolic acid 3-acetate treatment). AIF, apoptosis-inducing factor; PARP, poly(ADP-ribose) polymerase; SD, standard deviation.

suggesting that oleanolic acid 3-acetate effectively inhibits the growth of SKOV3 cells *in vivo* but has little, if any, toxicity toward the normal tissues.

4. Discussion

Oleanane triterpenoids are found in numerous plants and plant extracts including *Panax ginseng* Meyer. Owing to easy preparation and enriched biological activities, oleanane triterpenoid framework is yet to provide an interesting template for combinatorial and medicinal chemistry. Supporting this view are a certain number of oleanane triterpenoids that exhibit promising antiproliferative activities. In line with this view, we synthesized a novel oleanane triterpenoid, namely, oleanolic acid 3-acetate and explored its anticancer activity against ovarian cancer and endometrial cancer, two most frequently encountered gynecological cancers, with a hope to evaluate its anticancer efficacy and to elucidate underlying mechanisms for its anticancer activities.

It is interesting to note that higher mammals have evolved complex death pathways, many of which converge on apoptotic programs via the mitochondria as a key regulatory component [22]. Our data clearly supported the view that oleanolic acid 3-acetate has an anticancer activity by stimulating apoptotic cell death mainly mediated by mitochondrial dysfunction. Concentration-dependent abolition of $\Delta\Psi_m$, release of AIF and cytochrome c, and decrease in *Bcl*-2 all support the notion that oleanolic acid 3-acetate exerts its anticancer activity via a mitochondria-mediated pathway.

There are some issues, however, that need to be addressed pertaining to proper interpretation of the present study. Are the doses that we used a biological active dose rather than a maximum tolerated dose? In this study, the concentrations were 0–40 μM of oleanolic acid 3-acetate. Within these concentration ranges, oleanolic acid 3-acetate causes a concentration-dependent cytotoxicity, implying that the concentration tested may not be physiologically saturated or maximally tolerated in cancer cells. It is also well established that many good drugs have high affinities toward the target molecules in nM concentration range, especially when its target is a single protein [23]. We measured the cytotoxicity of oleanolic acid 3-actate as revealed by the MTT assay. The cytotoxicity as assessed by the MTT assay may reflect a massive structural or functional change subsequently to cumulative downstream events of apoptotic or necrotic signal cascades; in other words, accumulation of many subtle early events may lead to massive structural or functional changes, such as mitochondrial depolarization and DNA fragmentation before leading to cell death. Thus, at relatively high concentrations, either 20 or 40 μM, nonspecific actions exerted by oleanolic acid 3-acetate could not be carefully differentiated from genuine apoptotic events by the MTT assay. This possibility is more likely to explain why high concentrations of oleanolic acid 3-acetate cause cytotoxicity toward normal epithelial cells.

Generally, the generation of ROS induced by cancer chemotherapeutics triggers the mitochondrial pathways [11,24,25]. In contrast, some reports also point out apoptosis via mitochondrial pathway but independent of ROS generation [12,13]. Intriguingly, oleanolic acid 3-acetate decreased the cellular ROS level at the concentrations

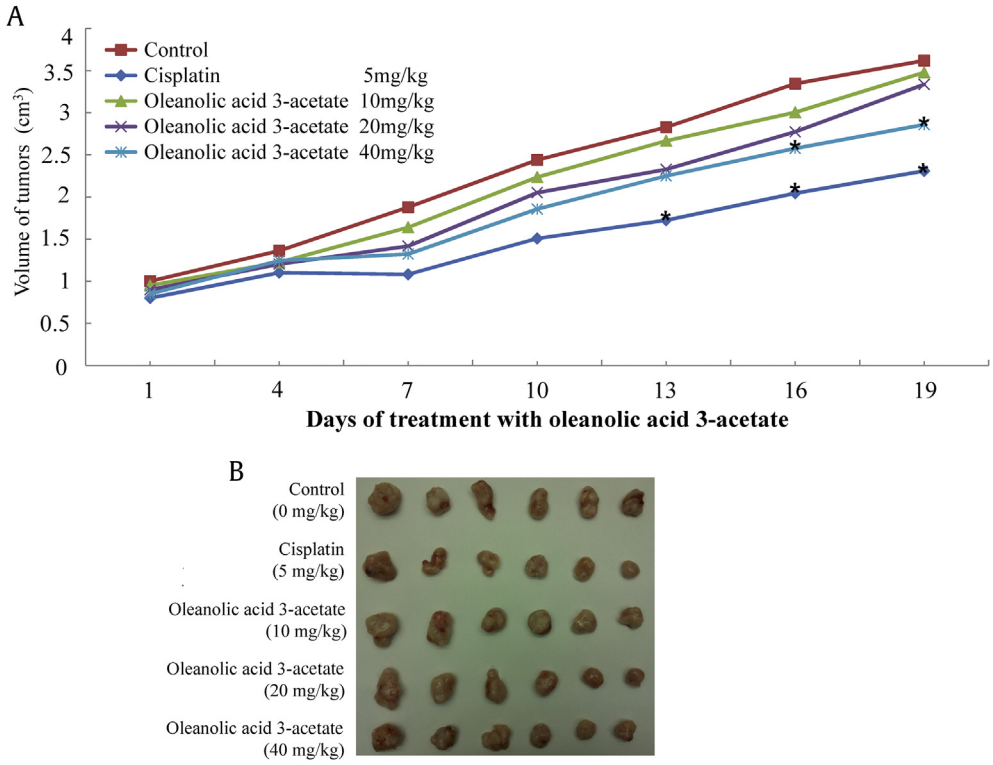

Fig. 5. Oleanolic acid 3-acetate inhibits the growth of SKOV3 cell xenografts in nude mice. The xenograft mice model for ovarian tumor was generated by implanting subcutaneously (*s.c.*) 5×10^6 of SKOV3 cells into the left flank of an athymic mouse. After the tumor size became visible (~3 weeks), mice were randomly divided into five groups before oleanolic acid 3-acetate was injected intraperitoneally (*i.p*). The negative control group mice were injected with 0.1% DMSO in saline; the positive control group mice were injected with 5 mg/kg of cisplatin; three different concentrations of oleanolic acid 3-acetate (10 mg/kg, 20 mg/kg, and 40 mg/kg) were injected. (A) Tumor volume was monitored externally by measuring the long and short axis of the tumor xenografts and calculated as described in *Materials and Methods*. Data were represented as means of 5 experimental animals. $^*p < 0.05$ versus control. (B) The excised tumors are displayed at the end of the experiment (Day 19).

Table 1
Inhibitory effects of oleanolic acid 3-acetate on the growth of SKOV3 cell xenografts in nude mice

Group	Before experiment		After experiment		Tumor weight (g)	Inhibition ratio (%)
	n	Body weight (g)	*n*	Body weight (g)		
Control	6	21.00 ± 0.34	6	22.75 ± 2.90	2.19 ± 0.88	
Cisplatin (5 mg/kg)	6	22.38 ± 0.89	6	20.78 ± 1.37	1.08 ± 0.51*	50.78
Oleanolic acid 3-acetate (10 mg/kg)	6	22.05 ± 1.01	6	22.91 ± 2.02	1.48 ± 0.46	32.50
Oleanolic acid 3-acetate (20 mg/kg)	6	21.58 ± 0.77	6	22.35 ± 0.98	1.35 ± 0.39*	38.47
Oleanolic acid 3-acetate (40 mg/kg)	6	21.64 ± 0.88	6	22.96 ± 0.75	1.18 ± 0.38*	46.02

SKOV3 cells were implanted *s.c.* under the left flanks of athymic mice. Animals were randomized into five groups and were treated with oleanolic acid 3-acetate by daily *i.p.* injection for 19 days: Control, treated with vehicle (0.1% DMSO diluted in saline); Cisplatin, treated with cisplastin at the dose of 5 mg/kg body weight (positive control); Oleanolic acid 3-acetate, treated with oleanolic acid 3-acetate at the dose of 10, 20, and 40 mg/kg body weight. The body weight of mice was measured every 3 days after initiating the treatment. The tumor weights were measured on sacrificing the mice at the 19th day after treatment. Data represented the means ± SD ($n = 6$). Tumor growth was significantly inhibited ($^*p < 0.05$ vs. the control).

used (0–40 μM) both in SKOV3 cells and HEC-1A cells. Our results strongly suggest that oleanolic acid 3-acetate triggers apoptotic cell death via a novel mitochondrion-dependent but ROS-independent pathway. Further studies are needed to clarify this seemingly conflicting novel pathway.

In conclusion, oleanolic acid 3-acetate effectively induced apoptotic cell death in SKOV3 cells and HEC-1A cells both *in vitro* and *in vivo*. Its underlying mechanism is mostly likely to be linked to an ROS-independent mitochondrial dysfunction. Therefore, oleanolic acid 3-acetate may be a promising new compound benefiting the cancer chemotherapy.

Conflicts of interest

The authors declare that there are no conflicts of interest.

Acknowledgments

The authors are grateful to Mr Jae Hoon Lee, Ajou University Hospital, Suwon, South Korea, for his technical advice. This work was supported by the Korean Research Foundation grant 2012R1A1B3000486 funded by the Korean Government (MEST).

References

[1] Hill RA, Connolly JD. Triterpenoids. Nat Prod Rep 2011;28:1087–117.
[2] Liby KT, Yore MM, Sporn MB. Triterpenoids and rexinoids as multifunctional agents for the prevention and treatment of cancer. Nat Rev Cancer 2007;7:357–69.
[3] Bray F, Jemal A, Grey N, Ferlay J, Forman D. Global cancer transitions according to the Human Development Index (2008-2030): a population-based study. Lancet Oncol 2012;13:709–801.

[4] Bolton KL. Role of common genetic variants in ovarian cancer susceptibility and outcome. J Intern Med 2012:1365–2796.
[5] Sjöblom T, Jones S, Wood LD, Parsons DW, Lin J, Barber TD, Mandelker D, Leary RJ, Ptak J, Sillman N, et al. The consensus coding sequences of human breast and colorectal cancers. Science 2006;314:268–74.
[6] Loeb LA. Human cancers express mutator phenotypes: origin, consequences and targeting. Nat Rev Cancer 2011;11:450–7.
[7] Jutooru I, Chadalapaka G, Abdelrahim M, Basha MR, Samudio I, Konopleva M, Andreeff M, Safe S. Methyl 2-cyano-3,12-dioxooleana-1,9-dien-28-oate decreases specificity protein transcription factors and inhibits pancreatic tumor growth: role of microRNA-27a. Mol Pharmacol 2010;78(2):226–36.
[8] Park WH, Lee MS, Park K, Kim ES, Kim BK, Lee YY. Monensin-mediated growth inhibition in acute myelogenous leukemia cells via cell cycle arrest and apoptosis. Int J Cancer 2001;101:235–42.
[9] Lin HI, Lee YJ, Chen BF, Tsai MC, Lu JL, Chou CJ, Jow GM. Involvement of Bcl-2 family, cytochrome c and caspase 3 in induction of apoptosis by beauvericin in human non-small cell lung cancer cells. Cancer Lett 2005;230:248–59.
[10] Campos CB, Degasperi GR, Pacífico DS, Alberici LC, Carreira RS, Guimarães F, Castilho RF, Vercesi AE. Ibuprofen-induced Walker 256 tumor cell death: cytochrome c release from functional mitochondria and enhancement by calcineurin inhibition. Biochem Pharmacol 2004;68:2197–206.
[11] Hu S, Zhao H, Al-Humadi NH, Yin XJ, Ma JK. Silica-induced apoptosis in alveolar macrophages: evidence of in vivo thiol depletion and the activation of mitochondrial pathway. J Toxicol Environ Health 2006;69:1261–84.
[12] Arimura T, Kojima-Yuasa A, Kennedy DO, Matsui-Yuasa I. Reactive oxygen species-independent G1 arrest induced by evening primrose extract in Ehrlich ascites tumor cells. Cancer Lett 2004;207:19–25.
[13] Ko CH, Shen SC, Hsu CS, Chen YC. Mitochondrial-dependent, reactive oxygen species-independent apoptosis by myricetin: roles of protein kinase C, cytochrome c, and caspase cascade. Biochem Pharmacol 2005;69:913–27.
[14] Flynn JM, Cammarata PR. Estradiol attenuates mitochondrial depolarization in polyol-stressed lens epithelial cells. Mol Vis 2006;12:271–82.
[15] Park DW, Choi DS, Ryu H-S, Kwon HC, Joo H, Min CK. A well-defined in vitro three-dimensional culture of human endometrium and its applicability to endometrial cancer invasion. Cancer Lett 2003;195:185–92.
[16] Choi DS, Kim JH, Ryu HS, Kim HC, Han JH, Lee JS, Min CK. Syndecan-1, a key regulator of cell viability in endometrial cancer. Int J Cancer 2007;121:741–50.
[17] Park DW, Cho T, Kim MR, Kim YA, Min CK, Hwang KJ. ATP-induced apoptosis of human granulosa luteal cells cultured in vitro. Fertil Steril 2003;80:993–1002.
[18] Oh JH, Lee HS, Park SH, Ryu HS, Min CK. Syndecan-1 overexpression promotes tumor growth and angiogenesis in an endometrial cancer xenograft model. Int J Gynecol Cancer 2010;20:751–6.
[19] Mendel DB, Laird AD, Xin X, Louie SG, Christensen JG, Li G, Schreck RE, Abrams TJ, Ngai TJ, Lee LB, et al. In vivo antitumor activity of SU11248, a novel tyrosine kinase inhibitor targeting vascular endothelial growth factor and platelet derived growth factor receptors: determination of a pharmacokinetic/pharmacodynamic relationship. Clin Cancer Res 2003;9:327–37.
[20] Joza N, Susin SA, Daugas E, Stanford WL, Cho SK, Li CYJ, Sasaki T, Elia AJ, Cheng HYM, Ravagnan L, et al. Essential role of the mitochondrial apoptosis-inducing factor in programmed cell death. Nature 2001;410:549–54.
[21] Wang XH, Jia DZ, Liang YJ, Yan SL, Ding Y, Chen LM, Shi Z, Zeng MS, Liu GF, Fu LW. Lgf-YL-9 induces apoptosis in human epidermoid carcinoma KB cells and multidrug resistant KBv200 cells via reactive oxygen species-independent mitochondrial pathway. Cancer Lett 2007;249:256–70.
[22] Park DS, Morris EJ, Stefanis L, Troy CM, Shelanski ML, Geller HM, Greene LA. Multiple pathways of neuronal death induced by DNA-damaging agents, NGF deprivation, and oxidative stress. J Neurosci 1998;18:830–40.
[23] Lambert DG. Drugs and receptors. Contin Edu Anesth Crit Care Pain 2004;4:181–4.
[24] Pae HO, Oh GS, Choi BM, Seo EA, Oh H, Shin MK, Kim TH, Kwon TO, Chung HT. Induction of apoptosis by 4-acetyl-12,13-epoxyl-9-trichothecene-3,15-diol from Isaria japonica Yasuda through intracellular reactive oxygen species formation and caspase-3 activation in human leukemia HL-60 cells. Toxicol In Vitro 2003;17:49–57.
[25] Zhuge J, Cederbaum AI. Serum deprivation-induced HepG2 cell death is potentiated by CYP2E1. Free Radic Biol Med 2006;40:63–74.